

OBSERVATIONS OF NOCTILUCENT CLOUDS IN THE WESTERN ARCTIC

Kazuyo Sakanoi⁽¹⁾, Richard L. Collins⁽²⁾, Yasuhiro Murayama⁽³⁾, Kohei Mizutani⁽³⁾

⁽¹⁾*Komazawa University, 1-23-1 Komazawa, Setagaya, Tokyo, 154-8525, JAPAN, ksakanoi@komazawa-u.ac.jp:*

⁽²⁾*Geophysical Institute, University of Alaska Fairbanks, 903 Koyukuk Drive, Fairbanks, AK 99775, USA, rlc@gi.alaska.edu:*

⁽³⁾*National Institute of Information and Communications Technology, 4-2-1 Nukui-kita, Koganei, Tokyo 184-8795, JAPAN, murayama@nict.go.jp, mizutani@nict.go.jp:*

ABSTRACT

This paper presents lidar and radar observations of the mesopause region during a visible noctilucent cloud (NLC) display at Chatanika, Alaska (65°N, 147°W) on the night of 9-10 August 2005. The lidar measurements reveal the evolution of a noctilucent cloud at 82.1 km. Simultaneous radar measurements provided wind measurements in the mesosphere. We discuss the evolution of the NLCs in terms of atmospheric gravity waves, the measured wind and current tidal models.

1. INTRODUCTION

The summer mesopause region (~80-100 km) is very cold with temperatures less than 150 K during the summer. These cold summer temperatures allow the formation of noctilucent clouds (NLCs) in the polar regions. NLCs (also termed polar mesospheric clouds) are composed of small water ice particles [1, 2].

NLCs were first reported in the late 19th century [3] and appear to have increased in frequency in the 20th century [4]. Models of the middle atmosphere indicate that the summer mesosphere should get colder as increases in greenhouse gas, carbon dioxide and methane, yield a colder middle atmosphere [5]. Based on these studies researchers have suggested that the polar summer mesosphere will become cloudier as more NLCs form (see [6], and references therein).

Only recently have routine lidar measurements of NLCs been established at polar sites (e.g., Scandinavia [7], Greenland [8], Antarctica [9], and Alaska [10]). Observational studies are limited by the seasonal occurrence (late-June to mid-August) of these clouds and their spatial and temporal patchiness. National Institute of Information and Communications Technology (NICT, Japan) Rayleigh Lidar was installed at Poker Flat Research Range, Chatanika, Alaska in November 1997[11]. NICT and the Geophysical Institute of the University of Alaska Fairbanks (USA) jointly operate the NICT Rayleigh lidar.

In this study we focus on lidar and digital camera observations on the night of 09-10 August 2005. In early August the nighttime solar depression angle was low enough ($> 7.7^\circ$ below the horizon) to yield lidar

measurements of both an NLC at 82.7 km and the mesospheric temperature profile (~40-80 km). We discuss the evolution of the NLC in terms of the influence of atmospheric gravity waves and background winds.

2. EXPERIMENT AND METHODS

The NICT Rayleigh lidar and MF (medium frequency) radar were installed at Poker Flat Research Range (PFRR), Chatanika, Alaska (65°N, 147°W) in November 1997 and October 1998 respectively. The NICT Rayleigh lidar is a single channel Rayleigh/Mie backscatter lidar [11]. The lidar has been employed to make measurements of temperature [12] and noctilucent clouds [10]. The raw lidar measurements yield profiles at 20 s and 75 m resolution. The lidar signal profiles is determined from the photon count profiles using standard techniques; four raw profiles are integrated, a 225 m running average is applied, the background signal is estimated and subtracted, and the signal is normalized to 1 at 70 km.

The NICT MF radar measures height profiles of horizontal wind velocity in the mesosphere and lower thermosphere throughout the day using partial reflection echoes from the ionospheric D region [13]. The raw MF radar measurements yield profiles at 3 minutes and 4 km resolution. Horizontal wind velocity is determined using the FCA (full correlation analysis) method [14]. In this paper we use horizontal wind profiles with 30-minute running average.

3. OBSERVATIONS

Observers on the ground noted the appearance of NLCs over the northern horizon early in the night and motion of the clouds southwestward towards the lidar observatory.

The strength of the lidar signal is an order of magnitude greater than those reported previously from Poker Flat Research Range. During 2322-0201 LST (=UT-9h) the lidar system recorded significant echoes from the NLC (Fig. 1). The solar depression angle was

more than 7.7° below the horizon after 2322 and more than 8.8° below the horizon until 0201. The average signal for this period shows the NLC with a peak altitude of 82.1 km and a peak signal of 3.6 corresponding to a backscatter ratio of 27-57 (assuming a pressure scale height of 4.5-6 km). Individual signal profiles show a peak altitude varying between 81.7 and 82.7 km with peak signals varying between 2.6 and 13.4 (Fig. 2).

NLC images were taken with a single-lens reflex digital camera every 1 minute throughout the night [15]. The NLC were visible from 0000 to 0250 LST and bulk motion of the NLC directed southwestward. Two wave-like structures in the NLC were seen from 0050 to 0225 LST (Fig 3). Distinct small scale waves with horizontal wavelength of ~ 50 km seemed to be frozen in a lower layer of the NLC and moved southwestward with NLC clouds, and obscure medium scale waves with horizontal wavelength of ~ 150 km propagated northeastward and seemed to exist in an upper layer. The phase front of small scale waves was almost perpendicular to that of the medium scale waves.

The horizontal wind velocity measured by the NICT MF radar is 0–50 m/sec southward and 20–75 m/sec

westward at altitude range of 76–84 km during 2300-0300 LST (0800-1200 UT) (Fig 4).

4. DISCUSSION

The two NLC layers were observed on the night of 9-10 August 2005 with the lidar and digital camera. The peak altitude of the individual lidar signal varied rapidly with peak-to-peak of ~ 1.5 km. The two wave-like structures were seen in the NLC images. These observations suggest that activity of atmospheric gravity waves (AGWs) was enhanced on the night, and that the evolution of NLCs would be caused by AGWs.

Coincidence of vertical motion of the two peaks of the lidar signal suggest that vertical wave length of AGWs, which would cause vertical motion of the two NLC peaks, was longer than an interval of the two peaks (~ 1 km). On the other hand, the small and medium scale AGWs in the NLC seemed to exist only in the lower and upper layer respectively. It suggests that vertical scale of those waves was very small less than ~ 1 km.

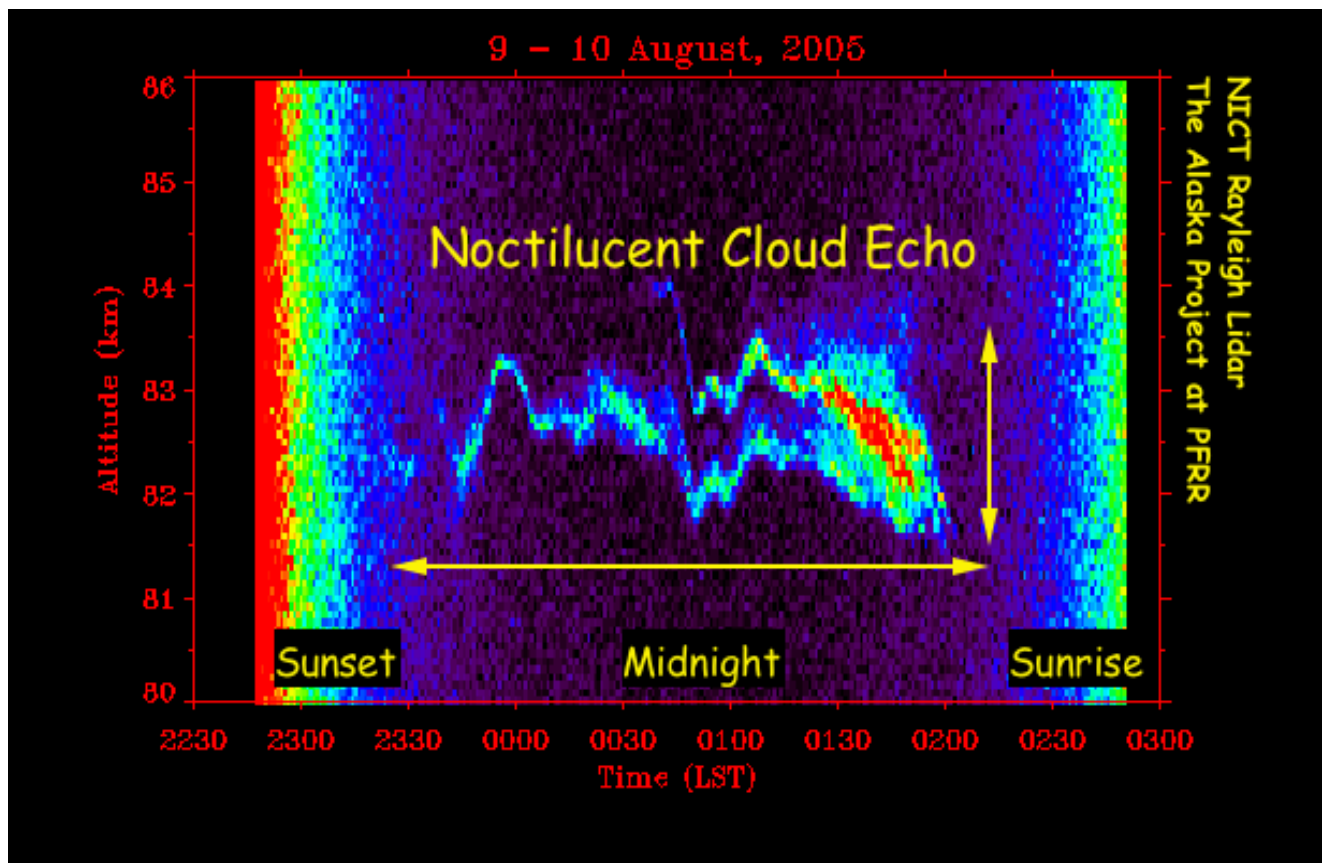


Fig. 1. Raw lidar photon count signal plotted as a function of local standard time (LST = UT – 9h) and altitude. The data is plotted on a grey scale with a maximum of 50 (white) and a minimum of 0 (black). The raw data is plotted as a resolution of 20 s and 75 m. Each profile represents the integrated signal from 1000 laser shots. The background signal is clearly visible decaying as the sun sets (before 2315) and increasing as the sun rises (after 0245). The NLC is clearly observed from 2330 until 0200. The cloud exists as a narrow single layer up to 0030, is observed as narrow double layers until 0130, and is observed as a broad single layer until 0200.

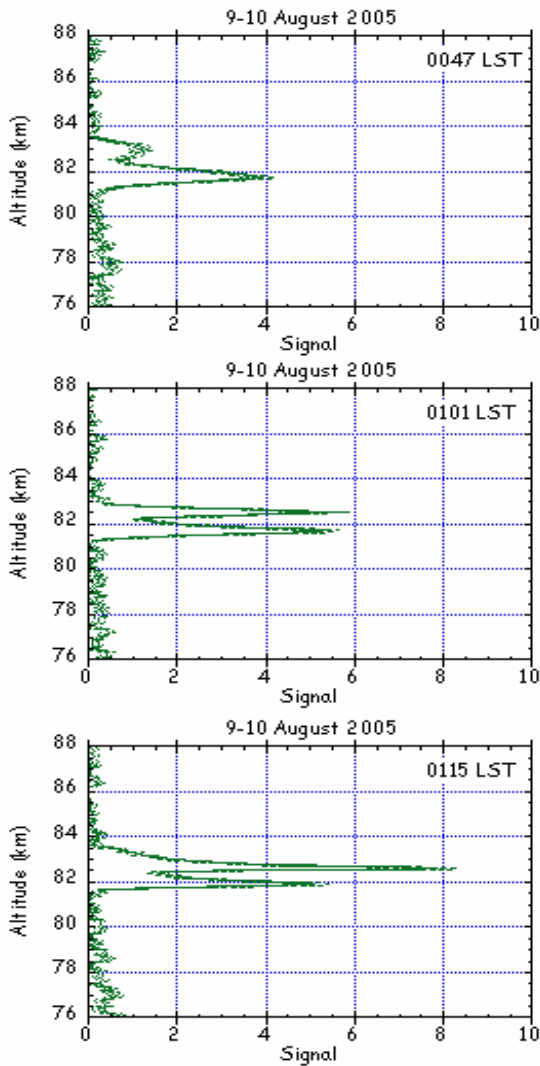


Fig. 2. Lidar signal profile plotted as a function of altitude. The dashed lines represent the one-sigma uncertainty in the signal due to the statistics of the photon counting process. Each profile represents the integrated echo of 4000 laser shots (80 s). The data is plotted at 75 m resolution and smoothed with a 225 m running average. The signal is normalized to 1 at 70 km

Strong southwestward wind measured with the NICT MF radar revealed that NLC clouds were advected by background winds. Southwestward motion of NLCs and strong southwestward winds are often observed over PFRR. The meridional wind measured by the radar during 8–11 August 2005 is shown in Fig. 4. Enhancement of southward wind of ~50m/s were observed diurnally during 2300-0300 LST (0800-1200 UT). Westward wind is dominant in summer over PFRR (not shown here).

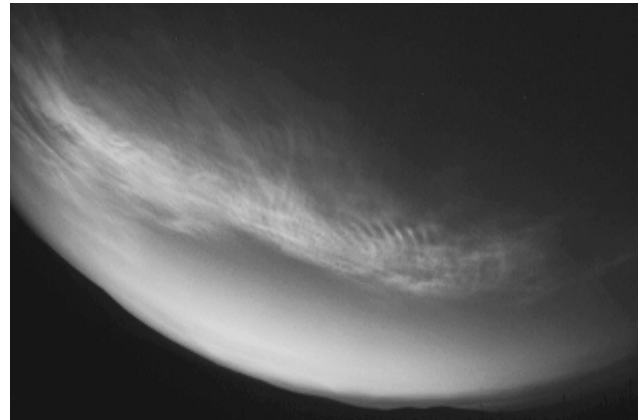


Fig 3. An image of NLC including wave-like structure over the northern horizon at 0139 LST on 10 August 2005.

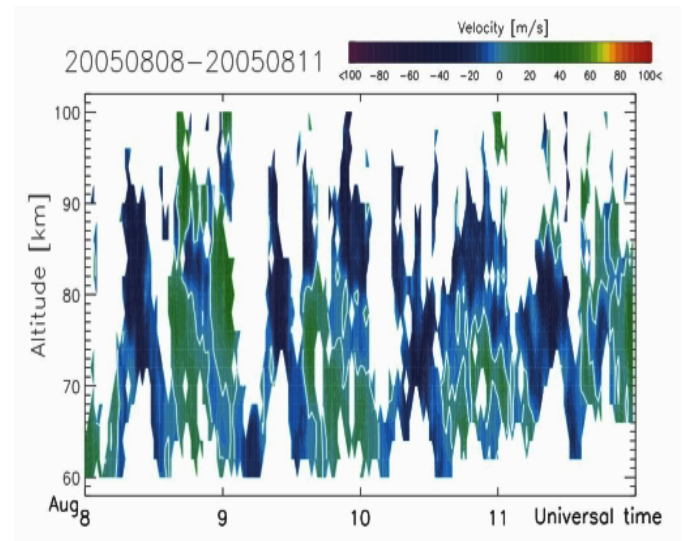


Fig 4. Meridional wind on 8 – 11 August 2005 plotted as a function of Universal time (UT = LST + 9h) and altitude (Grayish color: northward, black: southward).

We compare the measured diurnal enhancement of southward wind with the phase of diurnal and semidiurnal tides provided by Global Scale Wave Model (GSWM-02). The GSWM-02 was developed at High Altitude Observatory, National Center for Atmospheric Research (USA) and provides phase and amplitude of solar tides in the Earth's atmosphere from 0 - ~125 km on a web site (see [16, 17], and references therein). Southward winds of diurnal and semidiurnal tides are maximum at ~01 LST and ~23-04 LST respectively at

the altitude range of 76-86 km over PFRR. These results suggest that appearance and motion of NLCs observed at PFRR are affected with diurnal and semidiurnal tides.

5. CONCLUSIONS

We measured two NLC layers simultaneously with a Rayleigh lidar and digital camera on 09-10 August 2005 near local midnight. Rapid vertical motion of the lidar peaks and wave-like structures in NLC images were seen. These observations suggest that AGWs modulated peak altitude and horizontal structures of the NLC. Bulk motion of NLC clouds directed southwestward was observed. Horizontal wind measurements with an MF radar reveal that the bulk motion of the NLC was caused from the advection by enhanced background winds. The direction and occurrence time of the enhanced background winds are consistent with tidal winds calculated with the GSWM-02.

6. REFERENCES

1. von Cossart, et al., Size distribution of NLC particles as determined from three-color observations of NLC by groundbased lidar, *Geophys. Res. Lett.*, 26, 1513-1516, 1999.
2. Hervig, et al., First confirmation that water ice is the primary component of polar mesospheric clouds, *Geophys. Res. Lett.*, 28, 971-974, 2001.
3. Backhouse, T. W., The luminous cirrus cloud of June and July, *Meteorol. Mag.*, 20, 133, 1885.
4. Gadsden, M., and W. Schröder, *Noctilucent Clouds*, Springer-Verlag, Berlin, pp165, 1989.
5. Roble, R. G., and R. E. Dickinson, How will changes in carbon dioxide and methane modify the mean temperature structure of the mesosphere and thermosphere, *Geophys. Res. Lett.*, 16, 1441-1444, 1989
6. Thomas, G. E., Mesospheric clouds and the physics of the mesopause region, *Rev. of Geophys.*, 29, 553-575, 1991.
7. von Zahn, U., et al., the ALOMAR Rayleigh/Mie/Raman lidar: objectives configuration and performance, *Ann. Geophysicae*, 18, 815-833, 2000.
8. Thayer, J. P., et al., Noctilucent cloud observations over Greenland by a Rayleigh lidar, *Geophys. Res. Lett.*, 22, 2961-2964, 1995.
9. Chu, X., et al., Lidar observations of polar mesospheric cloud at the South Pole: Seasonal variations, *Geophys. Res. Lett.*, 28, 1203-1207, 2001.

10. Collins, R. L., et al., Simultaneous Lidar Observations of a Noctilucent Cloud and an Internal Wave in the Polar Mesosphere, *J. Geophys. Res.*, 108, 8435-84311, 2003.

11. Mizutani, K. et al., Rayleigh and Rayleigh Doppler Lidars for the Observations of the Arctic Middle Atmosphere, *IEICE Trans. Comms.*, E83-B, 2003, 2000.

12. Cutler, L. J. et al., Rayleigh Lidar Observations of Mesospheric Inversion Layers at Poker Flat, Alaska 67 °N, 147° W, *Geophys. Res. Lett.*, 28, 1467-1470, 2001.

13. Murayama, Y. et al., Medium Frequency Radars in Japan and Alaska for Upper Atmosphere Observations,

14. Briggs, B. H., The analysis of spaced sensor records by correlation techniques, *Handbook for MAP, vol.13*, 166-186, 1984. *IEICE Trans. Comms.*, E83-B, 1996, 2000.

15. http://salmon.nict.go.jp/awc/contents/index_e.php

16. Hagan, M. E. and J. M. Forbes, Migrating and nonmigrating semidiurnal tides in the upper atmosphere excited by tropospheric latent heat release, *J. Geophys. Res.*, 108(A2), 1062, doi:10.1029/2002JA009466, 2003

17. <http://web.hao.ucar.edu/public/research/tiso/gswm/gswm.html>

7. ACKNOWLEDGEMENTS

The study in this paper was conducted as a part of the National Institute of Information and Communications Technology Alaska Project. The authors thank the staff at Poker Flat Research Range for their ongoing support of the Alaska Project. The authors acknowledge the support of Jason G. McDonald, Zachary J. Marlow, Ligu Su, and Brentha Thurairajah in making the lidar observations. Poker Flat Research Range is operated by the Geophysical Institute with support from US National Aeronautics and Space Administration.